**An elegant four-helical fold in NOX and STEAP enzymes facilitates electron transport across biomembranes – similar vehicle, different destination**

Wout Oosterheert[1], Joana Reis[2], Piet Gros[1], Andrea Mattevi[2,*]

[1]Crystal and Structural Chemistry, Bijvoet Centre for Biomolecular Research, Department of Chemistry, Faculty of Science, Utrecht University, Padualaan 8, 3584 CH Utrecht, The Netherlands.

[2]Department of Biology and Biotechnology 'L. Spallanzani', University of Pavia, 27100 Pavia, Italy

*Correspondence: andrea.mattevi@unipv.it

Word count: 26 (Title and names) + 433 (Biographies) + 4009 (Main text) + 564 (Figure legends) = Total of 5032 words

**Conspectus**

The ferric-reductase superfamily comprises several oxidoreductases that use an intracellular electron source to reduce an extracellular acceptor substrate. NADPH oxidases (NOXs) and six-transmembrane epithelial antigen of the prostate enzymes (STEAPs) are iconic members of the superfamily. NOXs produce extracellular reactive oxygen species that exert potent bactericidal activities and trigger redox-signaling cascades that regulate cell division and differentiation. STEAPs catalyze the reduction of extracellular iron and copper which is necessary for the bioavailability of these essential elements. Both NOXs and STEAPs are present as multiple isozymes with distinct regulatory properties and physiological roles. Despite the important roles of NOXs and STEAPs in human physiology and despite their wide involvement in diseases like cancer, their mode-of-action at the molecular level remained incompletely understood for a long time, in part due to the absence of high-resolution models of the complete enzymes. Our two laboratories have elucidated the three-dimensional structures of NOXs and STEAPs, providing key insight into their mechanisms and evolution. The enzymes share a conserved transmembrane helical domain with an eye-catching hourglass shape. On the extracellular side, a heme prosthetic group is at the bottom of a pocket where the substrate ($O_2$ in NOX, chelated iron or copper in STEAP) is reduced. On the intracellular side, the inner heme of NOX and the FAD of STEAP are bound to topological equivalent sites. This is a rare case where critical amino acid substitutions and local conformational changes enable a cofactor (heme *vs* FAD) swap between two structurally and functionally conserved scaffolds. The catalytic core of these enzymes is completed by distinct cytosolic NADPH-binding domains that are topologically unrelated (a ferredoxin reductase-like flavoprotein domain in NOX and a $F_{420}H_2$:$NADP^+$-like domain in STEAP), feature different quaternary structures, and underlie specific regulatory mechanisms. Despite their differences, these domains all establish electron-transfer chains that direct the electrons from NADPH to the transmembrane domain. The multi-step nature of the process and the chemical nature of the products pose considerable problems in the enzymatic assays. We learned that great care must be exerted in the validation of a candidate inhibitor. Multiple orthogonal assays are required to rule out off-target effects such as ROS-scavenging activities or non-specific interference with the enzyme redox chain. The structural analysis of STEAP/NOX enzymes led us to further notice that their transmembrane heme-binding topology is shared by other enzymes. We found that the core domain of the cytochrome b subunits of the mitochondrial

complex III and photosynthetic cytochrome $b_6f$ are closely related to NOXs and STEAPs and likely arose from the same ancestor protein. This observation expands the substrate portfolio of the superfamily since cytochromes b act on ubiquinone. The rigidly packed helices of the NOX/STEAP/cytochrome b domain contrast with the more malleable membrane proteins like ion channels or amino-acid transporters, which undergo large conformational changes to allow passage of relatively large metabolites. This notion of a rigid hour-glass scaffold found an unexpected confirmation in the observation, revealed by structural comparisons, that an helical bundle identical to the NOX/STEAP/cytochrome b enzymes is featured by a *de novo* designed heme-binding protein, PS1. Apparently, nature and protein designers have independently converged to this fold as a versatile scaffold for heme-mediated reactions. The challenge is now to uncover the molecular mechanism that implement the isozyme-specific regulation of the enzyme functions and develop much-needed inhibitors and modulators for chemical biology and drug-design studies.

**Conspectus figure:**
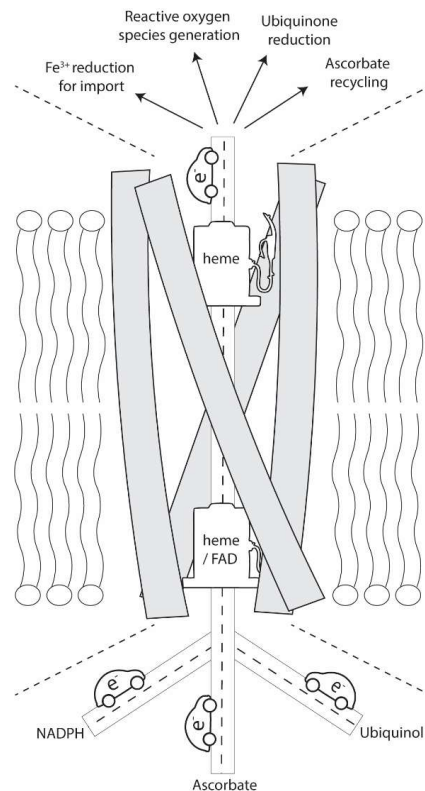
**Key references**

- Magnani, F.; Nenci, S.; Millana Fananas, E.; Ceccon, M.; Romero, E.; Fraaije, M. W.; Mattevi, A. Crystal Structures and Atomic Model of NADPH Oxidase. *Proc. Natl. Acad. Sci.* **2017**, *114*, 6764–6769.[1] *Crystal structures of the transmembrane and dehydrogenase domains of NOX5 yielded molecular insights into the structure and outer-sphere $O_2$-reduction mechanism of NADPH oxidases and provide potential sites for inhibitor design.*

- Oosterheert, W.; Bezouwen, L. S. Van; Rodenburg, R. N. P.; Granneman, J.; Förster, F.; Mattevi, A.; Gros, P. Cryo-EM Structures of Human STEAP4 Reveal Mechanism of Iron(III) Reduction. *Nat. Commun.* **2018**, *9*.[2] *This study provided a model for inter-subunit transmembrane-electron transport and iron(III) reduction by STEAPs through structures of human STEAP4, and also revealed that STEAPs require no accessory proteins to be enzymatically active.*

- Reis, J.; Massari, M.; Marchese, S.; Ceccon, M.; Aalbers, F. S.; Corana, F.; Valente, S.; Mai, A.; Magnani, F.; Mattevi, A. A Closer Look into NADPH Oxidase Inhibitors: Validation and Insight into Their Mechanism of Action. *Redox Biol.* **2020**, *32*.[3] *Enzymatic assays with multiple NOX isoforms show that numerous previously described NOX inhibitors in fact exhibit no NOX-inhibiting properties, and that great care must be undertaken to distinguish bona fide inhibitors from assay-interfering molecules.*

- Oosterheert, W.; Gros, P. Cryo-Electron Microscopy Structure and Potential Enzymatic Function of Human Six-Transmembrane Epithelial Antigen of the Prostate 1 ( STEAP1 ). *J. Biol. Chem.* **2020**, *295*, 9502–9512.[4] *Structural and functional experiments reveal that human STEAP1 is capable of reducing iron(III), suggest that it may have a regulatory role in STEAP-heterotrimers and show that antibodies can be used to inhibit the activity of STEAPs,.*

**Introduction**

The year 2020 marks the sixtieth anniversary of the publication of the structures of the heme-binding proteins myoglobin[5] and hemoglobin[6] by X-ray crystallography, representing the first ever elucidated three-dimensional models of proteins. This fundamental breakthrough, for which

John Kendrew and Max Perutz were awarded the Nobel Prize in Chemistry in 1962, ignited a new research field that focusses on understanding the function and mechanism of biomolecules by determining their atomic structure; nowadays known as structural biology[7]. Sixty years after the crystal structures of myoglobin and hemoglobin provided the first snapshots of how heme cofactors bind in a protein environment, the (bio)chemistry of heme-coordinating enzymes remains a prevalent theme of current day research. The unique chemical properties of hemes, combined with a variety of coordinating protein scaffolds, contribute to the diverse physiological functions observed for hemoproteins, which range from diatomic gas coordination to catalysis to electron transport[8]. Additionally, naturally occurring hemoproteins commonly serve as starting templates in directed evolution approaches to generate novel biocatalytic reactions that do not exist in nature[9], further emphasizing the versatility of hemes.

Hemoproteins are capable of catalyzing biological oxidoreductase reactions because the central heme iron adopts multiple oxidation states. For a subset of heme-dependent oxidoreductases, the oxidizing and reducing agents reside in separate cellular compartments. Hence, transmembrane-electron shuttling is required to enable the two half-reactions at opposite sides of a membrane, which is achieved by a specialized class of transmembrane oxidoreductases. These enzymes catalyze biochemical reactions by recruiting the redox substrates at either side of the membrane, and subsequently direct electron transport from one substrate to another through membrane-embedded heme cofactors. The maximum center-to-center distance between redox cofactors in proteins for functional single-step electron transfer is ~25 Å[10], whereas biological membranes typically span longer distances (>30 Å). As a result, electron transport through transmembrane oxidoreductases encompasses a multi-step electron-transfer cascade, a mechanism known as electron hopping[10–13].

**Commento [OW(1)]:** Reply 2.1

**Commento [OW(2)]:** Reply 1.1

The senior authors of this article did their PhD together at the University of Groningen (NL) in the early 90s. Thirty years later, their scientific interests crossed each other as their two labs became interested in two families of the transmembrane oxidoreductases, the NADPH oxidases (NOXs) and six-transmembrane epithelial antigen of the prostate enzymes (STEAPs). In this account, we provide a detailed analysis of the recent studies performed in our labs on the structure and mechanism of these evolutionary and functionally related enzymes. We then expand our analysis by comparing our work with structures of oxidoreductases that were

previously never described to be related to NOXs or STEAPs but share a similar heme-binding transmembrane core which facilitates 'across the membrane' redox reactions.

## Structural insights into NOX and STEAP enzymes

In 2017, the Mattevi laboratory reported the first crystal structures of the transmembrane domain and dehydrogenase domain of a NADPH oxidase (NOX)[1]. NOXs reduce $O_2$ to produce extracellular reactive oxygen species (ROS) involved in redox signaling, cell proliferation and antimicrobial and antifungal defense. Humans contain seven NOX enzymes, known as NOX1-5 and DUOX1-2[14–16]. Their activities are tightly controlled by their respective partner proteins and/or cellular stimuli (e.g. $Ca^{2+}$). Misregulation of these enzymes is associated with a variety of diseases, which include cancer and neuronal and muscular dystrophy[17]. The structures of *Cylindrospermum stagnale* NOX5 yielded a model that provides insights into the reductase mechanism of NOXs at the molecular level (Fig. 1a).

Approximately a year later, the Gros laboratory published the single-particle cryo-EM structure of homo-trimeric *human* six-transmembrane epithelial antigen of the prostate 4 (STEAP4)[2]. Although crystal structures of the intracellular dehydrogenase domains (also known as oxidoreductase domains) of human STEAP3 and rat STEAP4 had previously been reported[18,19], the cryo-EM structure of human STEAP4 represented the first structure of a STEAP protein that contains both its intracellular dehydrogenase domain and six-helical transmembrane domain (Fig. 1b). The STEAP family comprises four members in humans (STEAP1-4), of which STEAP2-4 are metalloreductases that reduce iron from the ferric ($Fe^{3+}$) to ferrous ($Fe^{2+}$) state and copper from the cupric ($Cu^{2+}$) to cuprous ($Cu^+$) state[19–21]. This process is a crucial step in the metal-uptake mechanism of mammalian cells, since metal importers exclusively recognize the reduced forms of iron and copper. Besides maintaining cellular metal homeostasis[22,23], STEAPs are highly upregulated in a wide variety of cancers[24–26], making STEAP enzymes promising novel therapeutic targets[27,28].

The distant homology between NOX and STEAP enzymes was first established by a bioinformatics analysis that reported similarities between the six-helical transmembrane domains of both enzyme classes[29]. A more comprehensive study subsequently showed that NOXs and STEAPs are part of the heme-containing transmembrane ferric-reductase domain (FRD) superfamily, which also comprises fungal and bacterial ferric reductases, as well as the bacterial

**Commento [OW(3)]:** Reply 3.1

**Commento [OW(4)]:** Reply 3.2

**Commento [OW(5)]:** Reply 1.4

**Commento [OW(6)]:** Reply 2.2

YedZ reductases[30]. To the best of our knowledge, the structures of *C. stagnale* NOX5 (Fig. 1a) and *human* STEAP4 (Fig. 1b) represent the first available atomic models of FRD superfamily members. Thus, it only recently became possible to analyze and compare these enzymes guided by a structural framework.
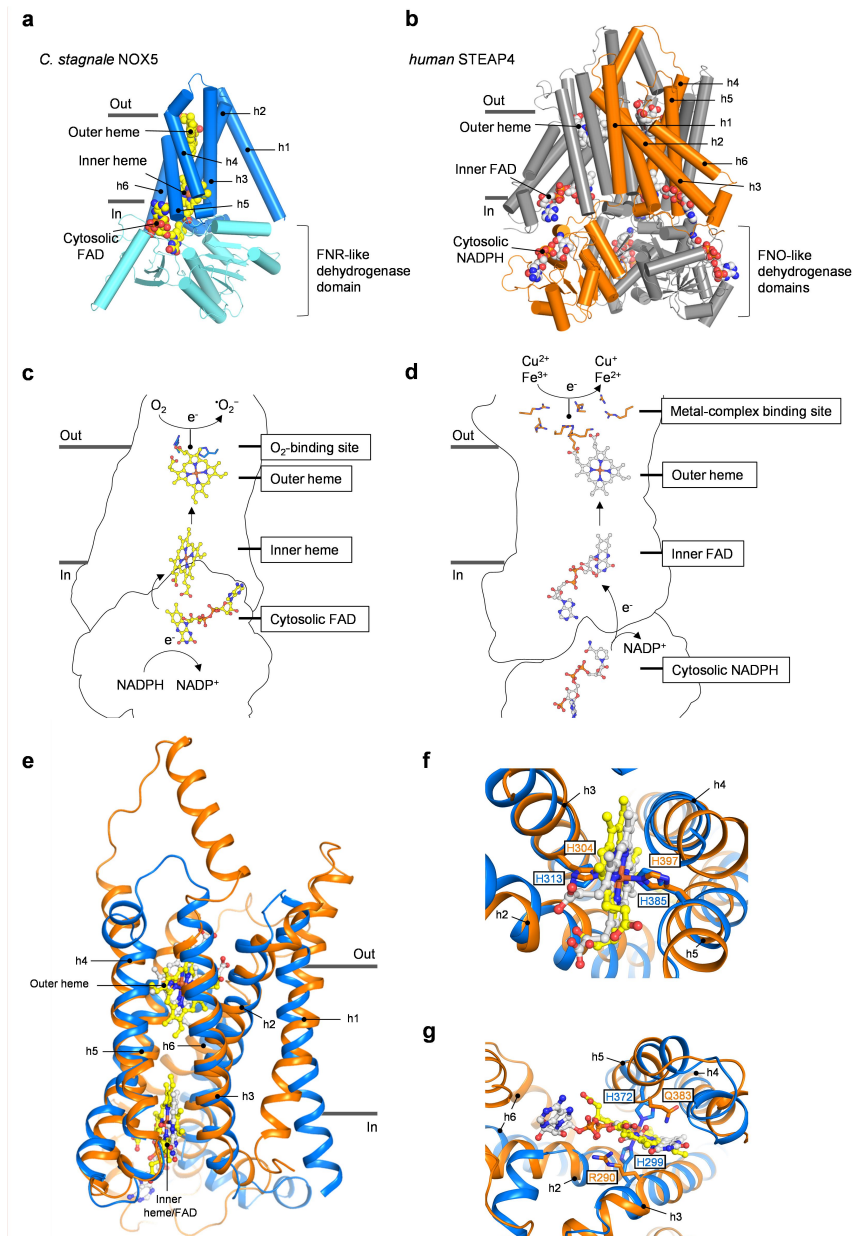
**Figure 1:** Structural comparison between NOX and STEAP enzymes. **(a)** Atomic model of *C. stagnale* NOX5 shown parallel to the membrane, based on structures of the dehydrogenase domain (cyan, pdb 5O0X) and transmembrane domain (blue, pdb 5O0T). Membrane helices and redox cofactors (carbon atoms yellow) are annotated. **(b)** Structure of trimeric *human* STEAP4 (pdb 6HCY) shown parallel to the membrane. One subunit is colored orange, whereas the other two subunits are depicted in grey. Membrane helices and redox cofactors (carbon

atoms white) are annotated. **(c)** Proposed transmembrane-electron transfer mechanism of NOX5. **(d)** Proposed transmembrane-electron transfer mechanism of STEAP4. **(e)** Superimposition of the transmembrane domains of NOX5 (blue) and STEAP4 (orange) viewed perpendicular to the membrane as sideview. Overlapping helices and cofactor-binding sites are annotated. **(f)** Overlay of the outer heme-binding pockets of NOX5 and STEAP4 viewed orthogonal to the membrane from the extracellular side. **(g)** Overlay of the binding sites of the inner heme in NOX5 and the inner FAD of STEAP4 viewed orthogonal to the membrane from the cytoplasmic side.

**A mosaic of domains**

NOXs and STEAPs both catalyze the transport of intracellular electrons to substrates at the opposite side of the membrane. However, when we compared the atomic models of NOX5 and STEAP4, it became evident that they differ in quaternary structure and exhibit a distinctive catalytic mode-of-action. The transmembrane and dehydrogenase domain crystal structures of NOX5 did not show evidence for physiologically-relevant oligomerization sites, whereas STEAP4 adopts a trimeric, domain-swapped architecture, arranged so that an intracellular domain resides beneath the transmembrane domain of the adjacent subunit (Fig. 1b). Mechanistically, NOXs and STEAPs utilize identical, non-covalently bound cofactor molecules to enable transmembrane-electron transport. However, the structures highlight critical differences in cofactor arrangement and binding stoichiometries (Fig. 1c, d). NOX5 coordinates the electron-donating substrate NADPH through a C-terminal ferredoxin-NADP$^+$ reductase-like (FNR-like) dehydrogenase domain. Electrons get passed on to an intracellularly-bound FAD cofactor, which releases them, one at a time, onto the transmembrane domain. Two axial heme-b ligands then transport the electron to the substrate $O_2$ at the membrane extracellular side (Fig. 1c). $O_2$ binds near the outer heme to be reduced, generating superoxide or hydrogen peroxide. Contrary to NOXs, STEAP4 recruits NADPH through an N-terminal $F_{420}H_2$:NADP$^+$-like (FNO-like) dehydrogenase domain, structurally unrelated to the FNR-like domain of NOXs. NADPH donates electrons to FAD that likely flips to anchor itself in the inner-membrane leaflet region of the adjacent STEAP subunit. Transmembrane-electron transport from FAD to $Fe^{3+}$ or $Cu^{2+}$-complexes advances through a single-heme cofactor bound in the outer-membrane leaflet side of the protein[31] (Fig. 1d). $Fe^{3+}$ and $Cu^{2+}$ bind as a complex with a negatively-charged chelator like citrate to a ring of basic amino acids positioned >6 Å above the heme. Both NOX5 and STEAP4 reduce their substrate without forming a covalent intermediate with the heme. Such an outer-sphere reduction mechanism is unique among known heme-depending proteins that typically function through a covalent intermediate between the heme-iron and the ligand/substrate.

9

In line with the obvious differences in the mechanism of both enzymes, NOX5 and STEAP4 share only 16% sequence identity in the region that spans membrane helices h2 – h5. Nevertheless, a structural superposition of both transmembrane domains reveals that helices h2 – h5 adopt a strikingly similar orientation and conformation (rmsd = 2.8 Å for 476 atoms), whereas helices h1 and h6 do not display a comparable orientation (Fig. 1e). Helices h2 – h5 are crucial for transmembrane-electron transport because they form the four-helical core that binds the di-heme motif in NOX5 and FAD-heme motif in STEAP4, respectively. An overlay of the four-helical cores at the extracellular-membrane leaflet side shows that the outer hemes reside at the same membrane depth and that the central-heme irons are coordinated by a pair of histidines located at equivalent positions in helices h3 and h5 (Fig. 1f). These histidine residues are strictly conserved in all NOX and STEAP homologs, as well as in all other members of the FRD superfamily[30], indicating a common mechanism for outer-heme binding. At the intracellular-membrane leaflet side of the four-helical core, the inner-heme binding site of NOX5 overlaps with the FAD-binding site of STEAP4 (Fig. 1g). Instead of two histidine residues that coordinate the inner heme of NOX5, STEAP4 harbors arginine and glutamine residues at the equivalent positions. The arginine and glutamine are strictly conserved in STEAP homologs and coordinate the phosphates and flavin ring of FAD, respectively. These structural observations confirm the findings from previous studies that STEAPs lost their second heme during evolution[30] and that the second heme-binding site diverged into a flavin-binding site[31], although the same four-helical core architecture to coordinate the cofactor is retained. Overall, we conclude that even though NOXs and STEAPs catalyze the reduction of different substrates, recruit NADPH through unrelated dehydrogenase domains, have a low-sequence identity, and display a different cofactor arrangement in their transmembrane domain, they share a highly similar heme-binding four-helical bundle to facilitate transmembrane-electron transport and reduction of their respective substrates, molecular oxygen and chelated metal ions ($Fe^{3+}$ or $Cu^{2+}$).

**Regulation of enzymatic activity**

As high levels of ROS lead to the damaging of DNA, proteins and lipids, the activity of NOXs needs to be tightly regulated. The dehydrogenase domain features a regulatory insertion sequence that contains a phosphorylation site that may serve as activity switch in human NOX2[32], and also represents a Hsp90-binding site in human NOX5[33]. Additionally, the C-

Commento [OW(11)]: Reply 1.6
Reply 3.1

terminal aromatic residue of the dehydrogenase domain needs to be displaced to allow for NADPH binding, which as we proposed may rely on conformational rearrangements of the surrounding protein scaffold[34]. NOX5 and DUOX1-2 furthermore contain an additional N-terminal regulatory domain, which inhibits their enzymatic activity when intracellular $Ca^{2+}$ levels are low[35]. Although far from completely understood, these examples highlight the complex, multilayered regulatory mechanisms underlying the activity of NOXs.

For STEAPs, a regulatory mechanism may exist through the formation of hetero-trimers between different STEAP paralogs. STEAP1, the first-identified member of the STEAP family that is highly upregulated in various types of cancer, lacks an intracellular dehydrogenase domain and does not exhibit ferric reductase activity when over-expressed in mammalian cells[21]. Although the physiological function of STEAP1 is unclear, the residues that coordinate FAD and heme in STEAP4 are conserved in the transmembrane domain of STEAP1. We solved the cryo-EM structure of STEAP1 bound to the antigen-binding fragment of an antibody (mAb120.545) used in anti-cancer clinical trials[4], revealing that the STEAP1 transmembrane domain is highly similar to the one of STEAP4 (Fig. 2). The proposed inter-subunit electron transport pathway in STEAP4 (Fig. 1d) indicates that STEAP1 may be a functional reductase in STEAP heterotrimers by receiving electrons from NADPH bound in the dehydrogenase domain of an adjacent STEAP2-4 subunit. Accordingly, we confirmed that the transmembrane domain of STEAP1 is capable of transmembrane electron transport and iron reduction in cells by generating a fusion protein containing the dehydrogenase domain of STEAP4 and transmembrane domain of STEAP1[4]. When taken together, these results suggest that the incorporation of STEAP1 into STEAP2-4 heterotrimers may dampen iron reduction rates locally by having fewer NADPH-binding sites available per trimer. It will be of interest to further investigate how cancer cells exploit these STEAP1-related regulatory mechanisms.
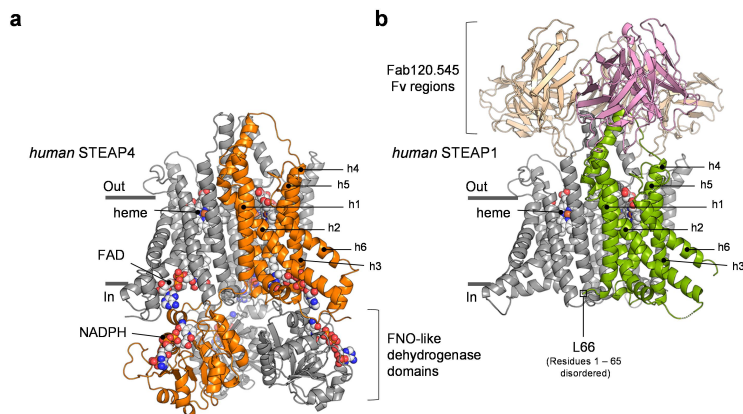
Commento [OW(12)]: Reply 2.3

**Figure 2:** STEAP paralogs adopt a highly similar transmembrane domain architecture. **(a, b)** Aligned structures of human STEAP4 (pdb 6HCY, panel **a**) and Fab120.545-bound human STEAP1 (pdb 6Y9B, panel **b**) shown parallel to the membrane. Two subunits per STEAP-trimer are grey, and one subunit is orange (STEAP4) or green (STEAP1). For the STEAP1-bound Fab120.545 Fv regions, one molecule is pink and the other two molecules are shown in yellow. Membrane helices and redox cofactors (carbon atoms white) are annotated.

## Ghostbusting in the search for NOX and STEAP inhibitors

NOXs are attractive pharmacological targets in immunomodulation, inflammation, fibrosis and cancer[36–39]. A NOX1/4 inhibitor (GKT137831) is currently in clinical trials for idiopathic pulmonary fibrosis[40]. There is a surging interest also in STEAPs as pharmacological targets in biological processes involving cell proliferation, apoptosis, and iron-related disorders[27,28]. A humanized variant of anti-STEAP1 monoclonal antibody 120.545, of which we solved the structure in complex with STEAP1 (Fig. 2b), is used in prostate cancer clinical trials as antibody-drug conjugate (termed DSTP3086S)[41] and as radiolabeled antibody (termed [89]Zr-DFO-MSTP2109A) for PET imaging[42,43]. Interestingly, our experiments have revealed that the antigen-binding fragment of antibody 120.545 inhibits the cellular ferric-reductase activity of a STEAP4/STEAP1 fusion protein in a concentration-dependent manner[4]. As the antibody-fragment binds in close vicinity to the putative substrate binding site in STEAP1, these initial results indicate that antibodies could represent general tools to modulate the activity of STEAPs, and potentially also NOXs.

The three-dimensional NOX and STEAP structures also suggest sites for small-molecule inhibitor design. A prime candidate would be the NADPH- and FAD-binding sites that would offer the possibility to halt the reaction at its earliest electron transfer step. Moreover, the $O_2$ and

chelated-metal binding sites would be attractive for their location on the outer side of the membrane, bypassing the needs for drugs that efficiently cross the membrane. Time will tell how the drug discovery will proceed by harnessing the structural knowledge.

These efforts towards inhibitor discovery and development remain, however, often hindered by the difficulties posed by the direct (NOX) and indirect (through Fenton reaction; STEAP) ROS-producing properties of these enzymes. A simple strategy to monitor enzyme activity is through NADPH consumption. However, performing a high-throughput screening can be a challenge considering the weak sensitivity of the assay due to the rather low molar extinction coefficient of NADPH ($\varepsilon_{340nm}$ = 6.22 mM$^{-1}$ cm$^{-1}$). Moreover, this assay can be problematic with compounds that are fluorescent or act as fluorescence quenchers. Recurrent screening workflows thereby often rely on methods that detect the reaction products, superoxide/hydrogen peroxide and soluble ferrous ion, respectively. For instance, 6-(4-methoxyphenyl)-2-methyl-imidazo[1,2-a]pyrazin-3(7H)-one (MCLA), sulfonated tetrazolium salt (WST-1), and cytochrome c are efficient sensors suited for detecting superoxide generation through chemiluminescence and spectrophotometry whereas coumarin-7-boronic acid (CBA) and the highly sensitive amplex red-peroxidase coupled assay are widely used to monitor $H_2O_2$ production[3,44–46]. Furthermore, electron spin resonance (ESR) spectroscopy might provide accurate data for the detection of ROS and ESR oximetry methodology can be employed for monitoring oxygen[47]. Electrochemical approaches for superoxide detection based on immobilized cytochrome c or superoxide dismutase biosensors can also be suitable for enzyme activity assessment[48]. An often-used protocol assay for ferrous iron detection employs ferrozine ($\varepsilon$ = 27.9 mM$^{-1}$cm$^{-1}$ for the $Fe^{2+}$-ferrozine complex) and chromogenic chelators[20,21,49]. All these assays (Fig. 3), however, are prone to artefacts and can easily yield false positives when searching and testing for inhibitors. It is therefore mandatory to run extensive control experiments that probe the validity of candidate hits. Enzymatic (e.g. xanthine oxidase) and non-enzymatic (e.g. NADH/phenazine methosulfate; fluorescein oxidation) assays should be used to check for any ROS-scavenging, antioxidant, electron-transfer, and Fe-reacting activities of a putative inhibitor[3,50–52]. Likewise, methods like microscale thermophoresis (MST) or surface plasmon resonance (SPR) designed to probe the direct binding to a protein are ultimately necessary to validate a compound. For instance, our workflow of NOX5 ligand screening comprises thermal shift assays and MST that helped us discriminate false positives from *bona-fide* NOX inhibitors. Orthogonal and control assays as

Commento [OW(13): Reply 1.3b

well as binding assays (Fig. 3) are also essential to detect pan-assay interference compounds (so-called *PAIN*s)[53] that can act as promiscuous ligands or interfere with some of the assays used (such is the case of catechols that easily scavenge ROS and often bear chemical structures able to bind several biological targets). In the informal conversations at meetings gathering the researchers in the field, it is often stated that "*one third of the Merck catalogue is redox reactive*". While we do not have any proof in support of this number, our hands-on experience has (somewhat painfully) taught us that many chemicals have indeed ROS-scavenging and/or assay-interfering activities. This fact should be carefully and critically considered when searching for ligands of NOXs and STEAPs.

| ASSAYS | NOXs | STEAPs | ADVANTAGES | DISADVANTAGES |
|---|---|---|---|---|
| *Direct enzymatic assay* | | | | |
| NADPH consumption | ✓ | ✓ | Used in absorbance or fluorescence; Less prone to interferences | Low sensitivity method; Better suited for purified enzyme |
| *Binding assay* | | | | |
| MST SPR | ✓ | ✓ | MST require low amounts of protein; SPR is label-free | SPR requires substantial protein amounts; Techniques are not high throughput |
| *Superoxide detection* | | | | |
| MCLA WST-1 Cytochrome C reduction | ✓ | ✗ | MCLA as a high throughput and sensitive chemiluminescence assay; WST-1 and cytochrome C are reliable and robust methods used in absorbance | MCLA chemical probe is subject to auto-oxidation; WST-1, and cytochrome c reduction assays have lower sensitivity |
| *Hydrogen peroxide detection* | | | | |
| Amplex red/peroxidase CBA | ✓ | ✗ | Sensitive and high throughput fluorometric assays | Peroxidase-dependent assays are prone to generate artefacts |
| *Iron detection* | | | | |
| Ferrozine | ✗ | ✓ | Specific colorimetric assay for iron detection | Low sensitivity False positives |
| **ROS scavenging detection** | | | | |

| *Enzymatic* | *Non – enzymatic* |
|---|---|
| Xanthine oxidase – amplex red/peroxidase | NADH-phenazine methosulfate HORAC |

**Figure 3:** Scheme of available assays for the screening of NOX and STEAP inhibitors.

## A widely conserved four-helical cofactor-binding fold

Inspired by the simplicity of the four-helical cofactor-binding module shared between NOX5 and STEAP4, we hypothesized that the fold, consisting of two antiparallel coiled coils, could represent a universal fold for coordinating cofactors that catalyze transmembrane-electron transfer. To identify other transmembrane enzymes that do not have an amino-acid sequence related to NOXs and STEAPs, but potentially share a similar fold, we searched for related structures with the DALI server[54], using the four-helical core models of NOX5 and STEAP4 as

14

references. We identified numerous transmembrane-oxidoreductase enzyme structures with significant structural similarities to the four-helical cores of NOXs and STEAPs, some of which were never related to NOX and STEAP enzymes before (Fig. 4c – f). Accordingly, the genes encoding for several of the identified proteins are termed 'cytochrome b', indicating that they bind a heme-b cofactor of which the central iron can adopt both ferrous and ferric oxidation states, consistent with an enzymatic function in electron transport. The hits that we analyzed further include: the eight-helical cytochrome b subunit that is part of the mitochondrial complex III[55], responsible for ubiquinol recycling in the Q-cycle of the electron transport chain[56], and of the related cytochrome b6f complexes that participate in photosynthesis[57] (Fig. 4c). Cytochrome b uses leftover electrons donated by ubiquinol ($QH_2$) to reduce ubiquinone (Q) and thereby replenish the ubiquinol pool for the reduction of cytochrome c. A second hit identified by our search is the six-helical duodenal ferric reductase dCytB[58,59], which reduces dietary iron for cellular uptake and is furthermore involved in ascorbate recycling (Fig. 4d). dCytB transfers electrons from intracellular ascorbate to ferric iron at the extracellular side of the membrane. Although dCytB enzymes exhibit a molecular function similar to that of STEAPs, they are not assigned to the FRD superfamily due to the absence of a matching sequence motif between dCytB and members of the FRD superfamily. The third structural homolog revealed by our analysis is the four-helical bacterial superoxide-oxidase, which scavenges reactive oxygen species from the periplasm and thus has a function microscopic-reverse to the ROS-generating NOXs (SOO, also known as cytochrome $b_{561}$, Fig. 4e)[60]. SOO enzymes are proposed to funnel electrons from periplasmic ROS to ubiquinone in the cytoplasm. The four-helical cytochrome b556 subunit of the bacterial formate dehydrogenase complex represents the last NOX/STEAP structural homolog identified by our search[61] (Fig. 4f). This complex is responsible for generating a proton-motive force by oxidizing formate to $CO_2$ in the periplasm. The electrons generated in this process tunnel through an array of iron-sulfur clusters to cytochrome b556, which transports them across the membrane to a quinone in the cytoplasm.

**Commento [OW(16):** Reply 2.4

**Commento [OW(17):** Reply 1.7

**Commento [OW(18):** Reply 2.5

**a**

*C. stagnale* NOX5
Helices h2 – h5

Reduction
Reaction: $O_2 \longrightarrow O_2^-$

Extracellular

Cytoplasm

Oxidation
Reaction: $NADPH \longrightarrow NADP^+$

**b**

*human* STEAP4
Helices h2-h5

$Cu^{2+} \longrightarrow Cu^+$
$Fe^{3+} \longrightarrow Fe^{2+}$

Endosome

Cytoplasm

$NADPH \longrightarrow NADP^+$

**c**

*human* cytochrome b
Helices h1-h4

$Q \longrightarrow Q^-$

Mitochondrial matrix

Inter-Membrane Space

$QH_2 \longrightarrow Q$

**d**

*human* dCytB
Helices h2 – h5

Reduction
Reaction: $Fe^{3+} \longrightarrow Fe^{2+}$

Extracellular

Cytoplasm

Oxidation
Reaction: Ascorbate $\longrightarrow$ Monodehydro-ascorbate

**e**

*E. coli* SOO
Helices h1 – h4

$Q \longrightarrow Q^-$

Cytoplasm

Periplasm

$O_2^- \longrightarrow O_2$

**f**

*E. coli* cytochrome b556
Helices h1 – h4

$Q \longrightarrow Q^-$

Cytoplasm

Periplasm

$HCOO^- \longrightarrow CO_2$

**g**

*A. xylosoxidans* cytochrome c'
Helices h1 – h4

**h**

*E. coli* cytochrome b562
Helices h1 – h4

**i**

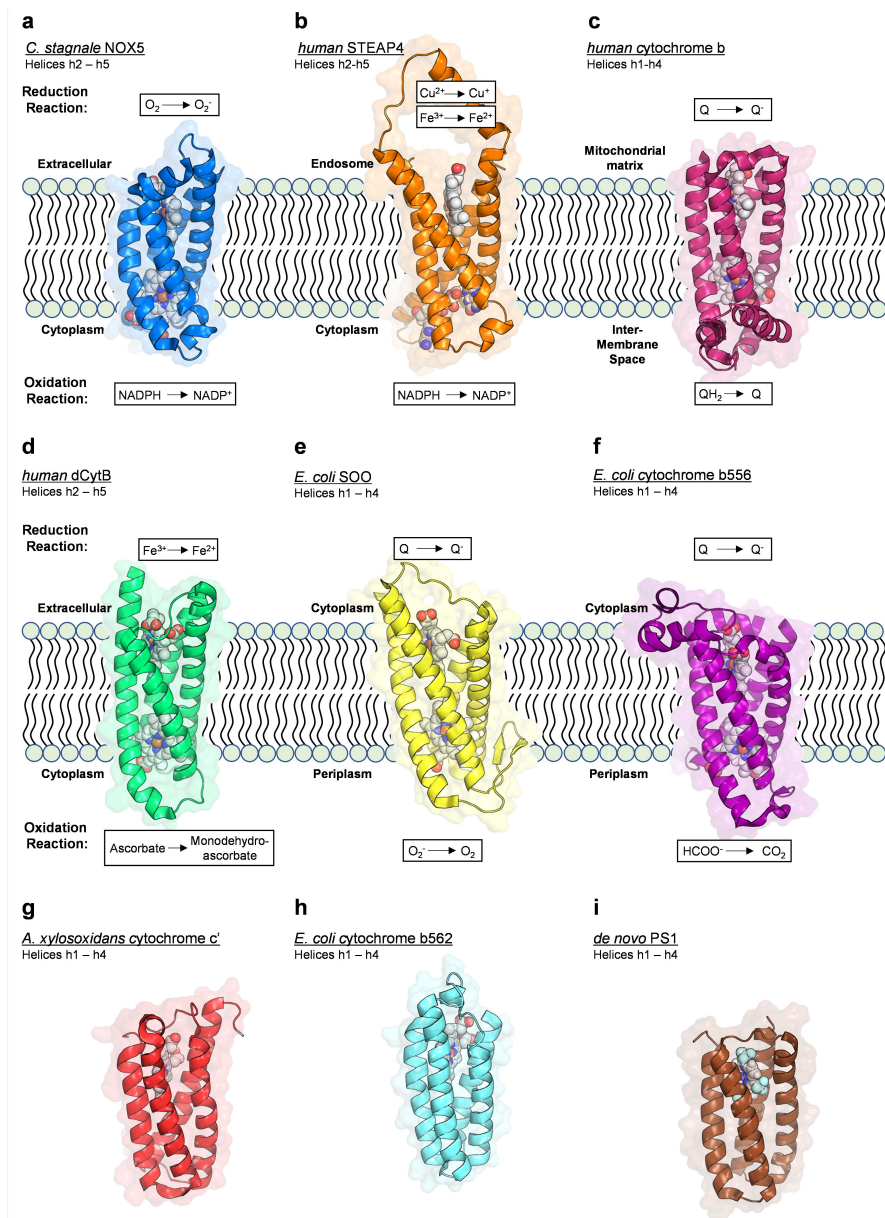*de novo* PS1
Helices h1 – h4

**Figure 4:** Cartoon representations of the architecture of the four-helical porphyrin-binding bundle in diverse classes of hemoproteins. All structures are aligned to the four-helical bundle of STEAP4. The transmembrane oxidoreductases are shown parallel to the membrane as a sideview with annotated topology. If applicable, the oxidative and reductive half reactions catalyzed by the hemoprotein are annotated. The depicted structures correspond to: **(a)** Residues 250 – 387 and the inner and outer heme b of *C. stagnale* NOX5 (blue, pdb 5O0t). **(b)** Residues 240 – 405 and the inner FAD and outer heme b of *human* STEAP4 (orange, pdb 6HCY). **(c)** Residues 28 –

201 and the inner and outer heme b of *human* cytochrome b (warmpink, pdb 5XTE). **(d)** Residues 43 – 186 and the inner and outer heme b of *human* dCytB (green, pdb 5ZLE). **(e)** Residues 6 – 161 and the inner and outer heme b of *E. coli* SOO (yellow, pdb 5OC0). **(f)** Residues 11 – 185 and the inner and outer heme b of *E. coli* cytochrome b556 (purple, pdb 1KQF). **(g)** Full-length *A. xylosoxidans* cytochrome c' bound to a single heme c (red, pdb 2XLE). **(h)** Residues 42 – 148 and the single heme b of *E. coli* cytchrome b562 (cyan, pdb 3U8P). **(i)** Full length, *de novo* designed PS1 bound to the non-natural porphyrin $(CF_3)_4PZn$ (brown, pdb 5TGY).

**Commento [OW(20]:** Reply 2.7

## Transmembrane-electron transport: differences, common features and principles

Generally, the above-identified enzymes catalyze processes in redox biology, ROS generation and scavenging, and iron metabolism. They all contain a right-handed, four-helical bundle transmembrane motif with similar inter-helical connections and bind two cofactors on both sides of the membrane (Fig. 4a - f). In agreement with the observation that STEAPs are the only transmembrane oxidoreductase enzymes that bind a single heme[31], all of the other enzyme structures discussed here harbor a di-heme motif in their transmembrane domain. The architecture of the common four-helical, cofactor-binding bundle resembles the shape of an hourglass, narrow in the center and wider on both sides of the membrane where the cofactors bind (Fig. 4a - f, Fig. 6). The orientation of the aligned four-helical bundles within the membrane is different and dependent on the total number of helices of the full-length enzymes. However, the proposed direction of electron transfer is the same in all proteins. Interestingly, despite the strong similarities in tertiary structure of the six enzymes, we observed no common fingerprint when comparing their amino acid sequences (Fig. 5). Thus, not a single amino acid residue is shared between all six structures at an equivalent position. For example, the outer-heme coordinating histidines reside in the second and fourth membrane helix in the four-helical bundle of NOX5, STEAP4, and cytochrome b, in the first and third helix of dCytB, and in the first and fourth helix of SOO and cytochrome b556. In addition, the distance between the redox cofactors bound in the four-helical bundle differs drastically between the enzymes (Fig. 6); the edge-to-edge distance between the inner and outer heme in NOX5 is 6.4 Å, whereas the distance between the hemes of dCytB is almost twice as large (12.3 Å). Combined, our sequence and structural analysis indicates that NOXs and STEAPs likely share a common ancestor with cytochrome $b_6$ of complex III in mitochondria. Conversely, NOXs and STEAPs appear to have evolved independently of dCytB, SOO and cytochrome b556. This strongly suggests that the structural resemblance observed for their four-helical porphyrin-binding bundles is a result of convergent

**Commento [OW(21]:** Reply 3.3b

**Commento [OW(22]:** Reply 2.6

17

evolution; the helical arrangement is an energetically favorable fold for coordinating a porphyrin, while retaining a stable conformation in the membrane.

Can we, besides the four-helical fold, identify other structural features shared by the enzymes that are crucial for efficient transmembrane-electron transport? In all compared structures, the hydrophobic residues residing in the membrane core between the two cofactors form a tightly packed inter-helical network, resulting in a compact and rigid architecture of the four-helical bundles (Fig. 6). In line with this, the X-ray and cryo-EM structures display low B-factors (or atomic displacement parameters) for residues in the transmembrane domains, indicating that these residues are highly ordered. Consequently, enzymes that perform transmembrane-electron transport exhibit a fundamentally different catalytic-mode of action compared to other proteins classes like ion channels or amino-acid transporters, which require large structural rearrangements to enable the transport of physical entities across biomembranes. Transmembrane-oxidoreductase enzymes instead facilitate the transport of electrons through tightly bound cofactors in a rigid, solvent inaccessible transmembrane domain; in other words, by keeping the electron-transfer path in place.
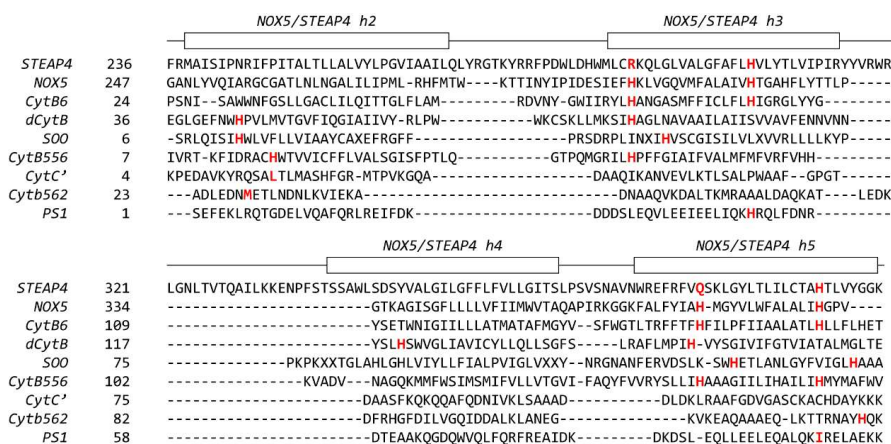


**Figure 5:** Sequence alignment based on DALI server structural superimpositions of the hemoproteins on the four-helical cofactor-binding bundle of STEAP4. Inserted segments compared to the STEAP4-sequence are hidden for clarification. The residues that coordinate or reside close to a cofactor are highlighted in red.
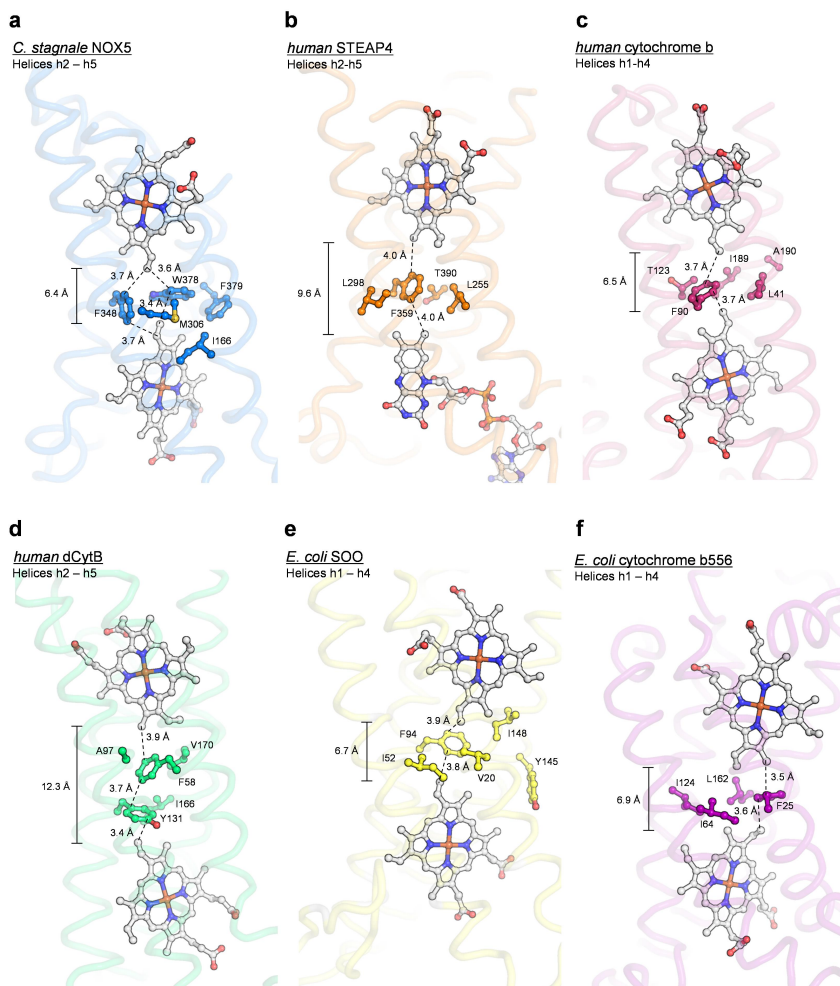
**Figure 6: (a - f)** Core packing of the four-helical cofactor-binding bundles of the membrane-embedded oxidoreductases. The amino acids that pack in between the cofactors are annotated, as well as the minimum edge to edge distance between the cofactors.

## Four-helical cofactor-binding folds in nature and beyond

Are there heme-binding soluble proteins that feature a helical bundle topologically similar to that of NOXs, STEAPS, cytochromes b? We found that this search criterion is matched only by a group of proteins comprising the bacterial cytochrome c' (pdb 2XLE) and cytochrome b562 (pdb 3U8P) (Fig. 4g, h). These four-helical bundle proteins reside in the periplasm where they are

thought to participate in electron transport through their single heme cofactors. The observation that the four-helical cofactor binding bundle is not more widely present in published structures of soluble proteins of higher order organisms indicates that the fold is not prevalent for soluble porphyrin-coordinating enzymes. In fact, more than thirty unique folds exist for soluble heme-binding proteins[62]. This wider variety in folds can be explained by the fact that numerous heme-coordinating conformations adopted by soluble proteins would not be compatible with a stable structure in the lipid bilayer, thereby limiting the number of protein arrangements that catalyze heme-mediated electron transport across a membrane.

In addition to these few natural occurring proteins, we also identified the structure of PS1[63] (Fig. 4i), a soluble, *de novo* designed porphyrin-binding four-helical bundle that has no significant sequence similarities with any known protein sequence found in nature. However, the experimentally determined NMR structure of PS1 bound to a non-natural porphyrin, in sub-Å agreement with the first-principles design, shares a highly similar fold with NOX5 (rmsd 2.8 Å for 98 aligned residues) and STEAP4 (rmsd 3.1 Å for 102 aligned residues). The PS1 study revealed that the design of a folded hydrophobic core of the four-helical bundle was essential to establish a highly stable cofactor binding site. When taken together, the strong structural similarities between *de novo* designed PS1 and biologically evolved NOX5 and STEAP4 provide further evidence that their four-helical bundle adopts an energetically favorable fold for coordinating a porphyrin.

**Commento [OW(25)]:** Reply 1.9

**Conclusions/Outlook**

With its elegant hourglass shape, the transmembrane helical bundle of the NOX/STEAP family of oxidoreductases can serve many functions. Its outer heme can direct electrons to diverse acceptors, such as molecular oxygen, ferric iron, and quinones. A distinct feature of this reaction is that it does not involve any covalent adduct with the heme iron, differently from the reactions catalyzed by heme proteins such as cytochrome P450s or the globins. As opposed to the close conservation of the transmembrane heme-binding scaffold, the cytosolic elements of these proteins are structurally diverse and unrelated. Their varying topologies feature characteristic quaternary structures, cofactor-binding sites and specificities, and regulatory elements. Despite the tremendous progress in the field, key questions remain open about the functioning of these enzymes. What are the structural mechanisms for the regulation of their enzymatic activities?

How did their isoform-specific properties evolve? How do they prevent the escape of electrons to the membrane milieu that could cause membrane-damaging lipid oxidation? Will powerful and selective drugs be identified? Behind their seemingly simple catalyzed reactions, these enzymes strike for the intricacy of their biology and the complexity of their functional mechanisms that are made possible by the distinct elements that decorate their conserved heme-binding scaffold.

**Biographies**

**Wout Oosterheert** received his B.S and M.S degrees in Chemistry 'cum laude' (highest distinction) from Utrecht University (the Netherlands). As part of his Master's curriculum, he spent seven months at Oregon Health & Science University in Portland OR (USA) to investigate the molecular principles of $P2X_3$ ion-channel gating using x-ray crystallography. In late 2015 he joined the structural biology lab of prof. Piet Gros at Utrecht University as a PhD candidate. Wout's research involves the structure and molecular mechanisms of transmembrane proteins that are upregulated in cancer, thereby focusing particularly on STEAP enzymes.

**Joana Reis** received her Chemistry B.S. and M.S degrees from Faculty of Sciences, University of Porto, Portugal. She completed her Medicinal Chemistry PhD fellowship in the University of Porto working on drug design applied to neurodegenerative diseases. In 2018, she joined Prof. Andrea Mattevi's group in the University of Pavia as a postdoctoral fellow with an Italian Association for Cancer Research and Marie Skłodowska-Curie grant. She is currently pursuing

the development of new NOX inhibitors and modulators as an approach to halt cancer cell proliferation.

**Piet Gros** obtained his Ph.D. in Structural Biology from Groningen University (The Netherlands) in 1990, supervised by Prof. Wim Hol. He was post-doctoral fellow at the ETH-Zurich (Switzerland) and Yale University (USA). In 1994, he started a protein-crystallography lab at Utrecht University (The Netherlands), where he became full professor in 2002 and distinguished faculty professor in 2018. His lab uses structural biology-techniques (crystallography and cryo-EM) to elucidate molecular mechanisms underlying biological processes with an emphasis of human plasma-proteins and cell-surface receptors. For his work on crystallography and the complement system he was elected member of the Dutch Royal Academy of Arts and Sciences (2010) and the European Molecular Biology Organization (2013); and, received the Gold Medal for life-time complement-research achievements (2017) and the Aminoff prize in Crystallography of the Royal Swedish Academy of Sciences (2018).

**Andrea Mattevi** obtained his Ph.D. in Structural Biology from Groningen University (The Netherlands) in 1992, supervised by Prof. Wim Hol. After that, he obtained a long-term EMBO-fellowship and worked as a post-doctoral fellow at the laboratory of molecular biology of the MRC (Cambridge, UK). In 1994, he became assistant-professor in the structural biology group at the University of Pavia (Italy) where he extended his enzymology research by redox enzymes in the context of complex mechanistic chemistry and drug design. He is now leading his structural biology research group at the same university and his research focuses on the molecular mechanisms of enzymes that use oxygen to either produce ROS in signaling networks, post-translationally modify histones, or transform metabolites and xenobiotics.

## References

(1)  Magnani, F.; Nenci, S.; Millana Fananas, E.; Ceccon, M.; Romero, E.; Fraaije, M. W.; Mattevi, A. Crystal Structures and Atomic Model of NADPH Oxidase. *Proc. Natl. Acad. Sci.* **2017**, *114*, 6764–6769.

(2)  Oosterheert, W.; Van Bezouwen, L. S.; Rodenburg, R. N. P.; Granneman, J.; Förster, F.; Mattevi, A.; Gros, P. Cryo-EM Structures of Human STEAP4 Reveal Mechanism of

Commento [OW(26)]: Reply E.2

Iron(III) Reduction. *Nat. Commun.* **2018**, *9*.

(3)  Reis, J.; Massari, M.; Marchese, S.; Ceccon, M.; Aalbers, F. S.; Corana, F.; Valente, S.; Mai, A.; Magnani, F.; Mattevi, A. A Closer Look into NADPH Oxidase Inhibitors: Validation and Insight into Their Mechanism of Action. *Redox Biol.* **2020**, *32*, 101466.

(4)  Oosterheert, W.; Gros, P. Cryo-Electron Microscopy Structure and Potential Enzymatic Function of Human Six-Transmembrane Epithelial Antigen of the Prostate 1 ( STEAP1 ). *J. Biol. Chem.* **2020**, *295*, 9502–9512.

(5)  Kendrew, J. C.; Dickerson, R.E.; Strandberg, B. E.; Hart, R. G.; Davies, D. R.; Phillips, D.C.; Shore, V. C. Structure of Myoglobin: A Three-Dimensional Fourier Synthesis at 2 A. Resolution. *Nature* **1960**, *185*, 422–427.

(6)  Perutz, M. F.; Rossmann, M. G.; Cullis, A. F.; Muirhead, H.; Will, G. Structure of Haemoglobin: A Three-Dimensional Fourier Synthesis at 5.5- A. Resolution, Obtained by X-Ray Analysis. *Nature* **1960**, *185*, 416–422.

(7)  Rossmann, M. G. The Beginnings of Structural Biology. *Protein Sci.* **1994**, *3*, 1731–1733.

(8)  Poulos, T. L. Heme Enzyme Structure and Function. *Chem. Rev.* **2014**, *114*, 3919–3962.

(9)  Chen, K.; Arnold, F. H. Engineering New Catalytic Activities in Enzymes. *Nat. Catal.* **2020**, *3*, 203–213.

(10)  Winkler, J. R.; Gray, H. B. Electron Flow through Metalloproteins. *Chem. Rev.* **2014**, *114*, 3369–3380.

(11)  Warren, J. J.; Ener, M. E.; Vlček, A.; Winkler, J. R.; Gray, H. B. Electron Hopping through Proteins. *Coord. Chem. Rev.* **2012**, *256*, 2478–2487.

(12)  Beratan, D. N.; Liu, C.; Migliore, A.; Polizzi, N. F.; Skourtis, S. S.; Zhang, P.; Zhang, Y. Charge Transfer in Dynamical Biosystems, or the Treachery of (Static) Images. *Acc. Chem. Res.* **2015**, *48*, 474–481.

(13)  Beratan, D. N. Why Are DNA and Protein Electron Transfer So Different? *Annu. Rev. Phys. Chem.* **2019**, *70*, 71–97.

(14)  Lambeth, J. D.; Neish, A. S. Nox Enzymes and New Thinking on Reactive Oxygen: A Double-Edged Sword Revisited. *Annu. Rev. Pathol. Mech. Dis.* **2014**, *9*, 119–145.

(15)  Magnani, F.; Mattevi, A. Structure and Mechanisms of ROS Generation by NADPH Oxidases. *Curr. Opin. Struct. Biol.* **2019**, *59*, 91–97.

(16)  Bedard, K.; Krause, K. H. The NOX Family of ROS-Generating NADPH Oxidases:

Physiology and Pathophysiology. *Physiol. Rev.* **2007**, *87*, 245–313.

(17)     Block, K.; Gorin, Y. Aiding and Abetting Roles of NOX Oxidases in Cellular
         Transformation. *Nat. Rev. Cancer* **2012**, *12*, 627–637.

(18)     Sendamarai, A. K.; Ohgami, R. S.; Fleming, M. D.; Lawrence, C. M. Structure of the
         Membrane Proximal Oxidoreductase Domain of Human Steap3, the Dominant
         Ferrireductase of the Erythroid Transferrin Cycle. *Proc. Natl. Acad. Sci. U. S. A.* **2008**,
         *105*, 7410–7415.

(19)     Gauss, G. H.; Kleven, M. D.; Sendamarai, A. K.; Fleming, M. D.; Lawrence, C. M. The
         Crystal Structure of Six-Transmembrane Epithelial Antigen of the Prostate 4 (Steap4), a
         Ferri/Cuprireductase, Suggests a Novel Interdomain Flavin-Binding Site. *J. Biol. Chem.*
         **2013**, *288*, 20668–20682.

(20)     Ohgami, R. S.; Campagna, D. R.; Greer, E. L.; Antiochos, B.; McDonald, A.; Chen, J.;
         Sharp, J. J.; Fujiwara, Y.; Barker, J. E.; Fleming, M. D. Identification of a Ferrireductase
         Required for Efficient Transferrin-Dependent Iron Uptake in Erythroid Cells. *Nat. Genet.*
         **2005**, *37*, 1264–1269.

(21)     Ohgami, R. S.; Campagna, D. R.; McDonald, A.; Fleming, M. D. The Steap Proteins Are
         Metalloreductases. *Blood* **2006**, *108*, 1388–1394.

(22)     Wellen, K. E.; Fucho, R.; Gregor, M. F.; Furuhashi, M.; Morgan, C.; Lindstad, T.;
         Vaillancourt, E.; Gorgun, C. Z.; Saatcioglu, F.; Hotamisligil, G. S. Coordinated
         Regulation of Nutrient and Inflammatory Responses by STAMP2 Is Essential for
         Metabolic Homeostasis. *Cell* **2007**, *129*, 537–548.

(23)     Zhou, J.; Ye, S.; Fujiwara, T.; Manolagas, S. C.; Zhao, H. Steap4 Plays a Critical Role in
         Osteoclastogenesis in Vitro by Regulating Cellular Iron/Reactive Oxygen Species (ROS)
         Levels and CAMP Response Element-Binding Protein (CREB) Activation. *J. Biol. Chem.*
         **2013**, *288*, 30064–30074.

(24)     Hubert, R. S.; Vivanco, I.; Chen, E.; Rastegar, S.; Leong, K.; Mitchell, S. C.; Madraswala,
         R.; Zhou, Y.; Kuo, J.; Raitano, a B.; Jakobovits, A.; Saffran, D. C.; Afar, D. E. STEAP: A
         Prostate-Specific Cell-Surface Antigen Highly Expressed in Human Prostate Tumors.
         *Proc. Natl. Acad. Sci. U. S. A.* **1999**, *96*, 14523–14528.

(25)     Grunewald, T. G. P.; Bach, H.; Cossarizza, A.; Matsumoto, I. The STEAP Protein Family:
         Versatile Oxidoreductases and Targets for Cancer Immunotherapy with Overlapping and

Distinct Cellular Functions. *Biol. Cell* **2012**, *104*, 641–657.

(26) Moreaux, J.; Kassambara, A.; Hose, D.; Klein, B. STEAP1 Is Overexpressed in Cancers: A Promising Therapeutic Target. *Biochem. Biophys. Res. Commun.* **2012**, *429*, 148–155.

(27) Gomes, I. M.; Maia, C. J.; Santos, C. R. STEAP Proteins: From Structure to Applications in Cancer Therapy. *Mol. Cancer Res.* **2012**, *10*, 573–587.

(28) Barroca-Ferreira, J.; Pais, J. P.; Santos, M. M.; Goncalves, A. M.; Gomes, I. M.; Sousa, I.; Rocha, S. M.; Passarinha, L. A.; Maia, C. J. Targeting STEAP1 Protein in Human Cancer: Current Trends and Future Challenges. *Curr. Cancer Drug Targets* **2017**, *18*, 222–230.

(29) Sanchez-pulido, L.; Rojas, A. M.; Valencia, A.; Martinez-a, C.; Andrade, M. A. ACRATA : A Novel Electron Transfer Domain Associated to Apoptosis and Cancer. *BMC Cancer* **2004**, *4*.

(30) Zhang, X.; Krause, K. H.; Xenarios, I.; Soldati, T.; Boeckmann, B. Evolution of the Ferric Reductase Domain (FRD) Superfamily: Modularity, Functional Diversification, and Signature Motifs. *PLoS One* **2013**, *8*.

(31) Kleven, M. D.; Dlakić, M.; Lawrence, C. M. Characterization of a Single B-Type Heme, FAD, and Metal Binding Sites in the Transmembrane Domain of Sixtransmembrane Epithelial Antigen of the Prostate (STEAP) Family Proteins. *J. Biol. Chem.* **2015**, *290*, 22558–22569.

(32) Beaumel, S.; Picciocchi, A.; Debeurme, F.; Vivès, C.; Hesse, A. M.; Ferro, M.; Grunwald, D.; Stieglitz, H.; Thepchatri, P.; Smith, S. M. E.; Fieschi, F.; José Stasia, M. Down-Regulation of NOX2 Activity in Phagocytes Mediated by ATM-Kinase Dependent Phosphorylation. *Free Radic. Biol. Med.* **2017**, *113*, 1–15.

(33) Chen, F.; Haigh, S.; Yu, Y.; Benson, T.; Wang, Y.; Li, X.; Dou, H.; Bagi, Z.; Verin, A. D.; Stepp, D. W.; Csanyi, G.; Chadli, A.; Weintraub, N. L.; Smith, S. M. E.; Fulton, D. J. R. Nox5 Stability and Superoxide Production Is Regulated by C-Terminal Binding of Hsp90 and CO-Chaperones. *Free Radic. Biol. Med.* **2015**, *89*, 793–805.

(34) Magnani, F.; Mattevi, A. Structure and Mechanisms of ROS Generation by NADPH Oxidases. *Curr. Opin. Struct. Biol.* **2019**, *59*, 91–97.

(35) Bánfi, B.; Tirone, F.; Durussel, I.; Knisz, J.; Moskwa, P.; Molnár, G. Z.; Krause, K. H.; Cox, J. A. Mechanism of Ca2+ Activation of the NADPH Oxidase 5 (NOX5). *J. Biol. Chem.* **2004**, *279*, 18583–18591.

(36)  Zhang, Y.; Murugesan, P.; Huang, K.; Cai, H. NADPH Oxidases and Oxidase Crosstalk in Cardiovascular Diseases: Novel Therapeutic Targets. *Nat. Rev. Cardiol.* **2020**, *17*, 170–194.

(37)  Ju, H. Q.; Ying, H.; Tian, T.; Ling, J.; Fu, J.; Lu, Y.; Wu, M.; Yang, L.; Achreja, A.; Chen, G.; Zhuang, Z.; Wang, H.; Nagrath, D.; Yao, J.; Hung, M. C.; DePinho, R. A.; Huang, P.; Xu, R. H.; Chiao, P. J. Mutant Kras- and P16-Regulated NOX4 Activation Overcomes Metabolic Checkpoints in Development of Pancreatic Ductal Adenocarcinoma. *Nat. Commun.* **2017**, *8*.

(38)  Singel, K. L.; Segal, B. H. NOX2-Dependent Regulation of Inflammation. *Clin. Sci.* **2016**, *130*, 479–490.

(39)  Amara, N.; Goven, D.; Prost, F.; Muloway, R.; Crestani, B.; Boczkowski, J. NOX4/NADPH Oxidase Expression Is Increased in Pulmonary Fibroblasts from Patients with Idiopathic Pulmonary Fibrosis and Mediates TGFβ1-Induced Fibroblast Differentiation into Myofibroblasts. *Thorax* **2010**, *65*, 733–738.

(40)  Green, D. E.; Murphy, T. C.; Kang, B. Y.; Kleinhenz, J. M.; Szyndralewiez, C.; Page, P.; Sutliff, R. L.; Hart, C. M. The Nox4 Inhibitor GKT137831 Attenuates Hypoxia-Induced Pulmonary Vascular Cell Proliferation. *Am. J. Respir. Cell Mol. Biol.* **2012**, *47*, 718–726.

(41)  Danila, D. C.; Szmulewitz, R. Z.; Vaishampayan, U.; Higano, C. S.; Baron, A. D.; Gilbert, H. N.; Brunstein, F.; Milojic-Blair, M.; Wang, B.; Kabbarah, O.; Mamounas, M.; Fine, B. M.; Maslyar, D. J.; Ungewickell, A.; Scher, H. I. Phase I Study of DSTP3086S, an Antibody-Drug Conjugate Targeting Six-Transmembrane Epithelial Antigen of Prostate 1, in Metastatic Castration-Resistant Prostate Cancer. *J. Clin. Oncol.* **2019**, *37*, 3518–3527.

(42)  O'Donoghue, J. A.; Danila, D. C.; Pandit-Taskar, N.; Beylergil, V.; Cheal, S. M.; Fleming, S. E.; Fox, J. J.; Ruan, S.; Zanzonico, P. B.; Ragupathi, G.; Lyashchenko, S. K.; Williams, S. P.; Scher, H. I.; Fine, B. M.; Humm, J. L.; Larson, S. M.; Morris, M. J.; Carrasquillo, J. A. Pharmacokinetics and Biodistribution of a [ 89 Zr]Zr-DFO-MSTP2109A Anti-STEAP1 Antibody in Metastatic Castration-Resistant Prostate Cancer Patients . *Mol. Pharm.* **2019**, *16*, 3083–3090.

(43)  Carrasquillo, J. A.; Fine, B.; Pandit-Taskar, N.; Larson, S. M.; Fleming, S.; Fox, J. J.; Cheal, S. M.; O'Donoghue, J. A.; Ruan, S.; Ragupathi, G.; Lyashchenko, S. K.; Humm, J. L.; Scher, H. I.; Gonen, M.; Williams, S.; Danila, D. C.; Morris, M. J. Imaging Metastatic

Castration-Resistant Prostate Cancer Patients with [89]Zr-DFO-MSTP2109A Anti-STEAP1 Antibody. *J. Nucl. Med.* **2019**, jnumed.118.222844.

(44) Augsburger, F.; Filippova, A.; Rasti, D.; Seredenina, T.; Lam, M.; Maghzal, G.; Mahiout, Z.; Jansen-Dürr, P.; Knaus, U. G.; Doroshow, J.; Stocker, R.; Krause, K. H.; Jaquet, V. Pharmacological Characterization of the Seven Human NOX Isoforms and Their Inhibitors. *Redox Biol.* **2019**, *26*, 101272.

(45) Zielonka, J.; Hardy, M.; Michalski, R.; Sikora, A.; Zielonka, M.; Cheng, G.; Ouari, O.; Podsiadły, R.; Kalyanaraman, B. Recent Developments in the Probes and Assays for Measurement of the Activity of NADPH Oxidases. *Cell Biochem. Biophys.* **2017**, *75*, 335–349.

(46) Miller, F. J.; Griendling, K. K. *Functional Evaluation of Nonphagocytic NAD(P)H Oxidases*; Elsevier Masson SAS, 2002; Vol. 353.

(47) He, W.; Liu, Y.; Wamer, W. G.; Yin, J. Electron Spin Resonance Spectroscopy for the Study of Nanomaterial-Mediated Generation of Reactive Oxygen Species. *J. Food Drug Anal.* **2014**, *22*, 49–63.

(48) Chen, X. J.; West, A. C.; Cropek, D. M.; Banta, S. Detection of the Superoxide Radical Anion Using Various Alkanethiol Monolayers and Immobilized Cytochrome C. *Anal. Chem.* **2008**, *80*, 9622–9629.

(49) Hirayama, T.; Nagasawa, H. Chemical Tools for Detecting Fe Ions. *J. Clin. Biochem. Nutr.* **2017**, *60*, 39–48.

(50) Hirano, K.; Chen, W. S.; Chueng, A. L. W.; Dunne, A. A.; Seredenina, T.; Filippova, A.; Ramachandran, S.; Bridges, A.; Chaudry, L.; Pettman, G.; Allan, C.; Duncan, S.; Lee, K. C.; Lim, J.; Ma, M. T.; Ong, A. B.; Ye, N. Y.; Nasir, S.; Mulyanidewi, S.; Aw, C. C.; Oon, P. P.; Liao, S.; Li, D.; Johns, D. G.; Miller, N. D.; Davies, C. H.; Browne, E. R.; Matsuoka, Y.; Chen, D. W.; Jaquet, V.; Rutter, A. R. Discovery of GSK2795039, a Novel Small Molecule NADPH Oxidase 2 Inhibitor. *Antioxidants Redox Signal.* **2015**, *23*, 358–374.

(51) Ponti, V.; Dianzani, M. U.; Cheeseman, K.; Slater, T. F. Studies on the Reduction of Nitroblue Tetrazolium Chloride Mediated through the Action of NADH and Phenazine Methosulphate. *Chem. Biol. Interact.* **1978**, *23*, 281–291.

(52) Ou, B.; Hampsch-Woodill, M.; Flanagan, J.; Deemer, E. K.; Prior, R. L.; Huang, D. Novel

Fluorometric Assay for Hydroxyl Radical Prevention Capacity Using Fluorescein as the Probe. *J. Agric. Food Chem.* **2002**, *50*, 2772–2777.

(53)   Baell, J. B.; Nissink, J. W. M. Seven Year Itch: Pan-Assay Interference Compounds (PAINS) in 2017 - Utility and Limitations. *ACS Chem. Biol.* **2018**, *13*, 36–44.

(54)   Holm, L. Structural Bioinformatics Benchmarking Fold Detection by DaliLite v . 5. *Bioinformatics* **2019**, 1–2.

(55)   Guo, R.; Zong, S.; Wu, M.; Gu, J.; Yang, M. Architecture of Human Mitochondrial Respiratory Megacomplex I2III2IV2. *Cell* **2017**, *170*, 1247-1257.e12.

(56)   Mitchell, P. Protonmotive Redox Mechanism of the Cytochrome B-C1 Complex in the Respiratory Chain: Protonmotive Ubiquinone Cycle. *FEBS Lett.* **1975**, *56*, 1–6.

(57)   Stroebel, D.; Choquet, Y.; Popot, J.; Picot, D. An Atypical Haem in the Cytochrome b 6 f Complex. **2003**, 413–418.

(58)   Lu, P.; Ma, D.; Yan, C.; Gong, X.; Du, M.; Shi, Y. Structure and Mechanism of a Eukaryotic Transmembrane Ascorbate-Dependent Oxidoreductase. *Proc. Natl. Acad. Sci. U. S. A.* **2014**, *111*, 1813–1818.

(59)   Ganasen, M.; Togashi, H.; Takeda, H.; Asakura, H.; Tosha, T.; Yamashita, K.; Hirata, K.; Nariai, Y.; Urano, T.; Yuan, X.; Hamza, I.; Mauk, A. G.; Shiro, Y.; Sugimoto, H.; Sawai, H. Structural Basis for Promotion of Duodenal Iron Absorption by Enteric Ferric Reductase with Ascorbate. *Commun. Biol.* **2018**, *1*.

(60)   Lundgren, C. A. K.; Sjöstrand, D.; Biner, O.; Bennett, M.; Rudling, A.; Johansson, A.; Brzezinski, P.; Carlsson, J.; Ballmoos, C. Von; Högbom, M. Scavenging of Superoxide by a Membrane-Bound Superoxide Oxidase. *Nat. Chem. Biol.* **2018**, *14*, 788–793.

(61)   Jormakka, M.; Törnroth, S.; Byrne, B.; Iwata, S. Molecular Basis of Proton Motive Force Generation: Structure of Formate Dehydrogenase-N. *Science (80-. ).* **2002**, *295*, 1863–1868.

(62)   Li, T.; Bonkovsky, H. L.; Guo, J. T. Structural Analysis of Heme Proteins: Implication for Design and Prediction. *BMC Struct. Biol.* **2011**, *11*.

(63)   Polizzi, N. F.; Wu, Y.; Lemmin, T.; Maxwell, A. M.; Zhang, S.; Rawson, J.; Beratan, D. N.; Therien, M. J.; Degrado, W. F. De Novo Design of a Hyperstable Non-Natural Protein–Ligand Complex with Sub-Å Accuracy Nicholas. *Nat. Chem.* **2017**, *9*, 1157–1164.